J Fluoresc (2014) 24:1055–1059
DOI 10.1007/s10895-014-1384-1

ORIGINAL PAPER

Analysis of Cytosolic pH Changes in Thymocytes During Early Apoptosis with Improved Three-Channel Real-Time Fluorescence Imaging

Zhang Shu · Liu Xiaochen · Deng Chuyun · Han Man · Pan Juhua · Liao Xinghua · Qi Xin · Duan Shaojin · Ma Wanyun

Received: 3 December 2013 / Accepted: 24 March 2014 / Published online: 17 April 2014

Abstract Cytosolic pH changes in single thymocytes in the early stages of apoptosis were examined with spectral-crosstalk-improved three-channel real-time fluorescence imaging. Spectral crosstalk was greatly reduced by this improved image processing method. Compared with normal thymocytes, the improved image processing method showed that the cytosolic pH value of thymocytes undergoing apoptosis was lower. A slight diversity in the intracellular pH values of samples subjected to different drug treatments was also observed. This new image processing method is beneficial to the application of the three-channel real-time fluorescence imaging to biological processes.

Keywords Three-channel · Spectral crosstalk · Real-time fluorescence imaging · Apoptosis · Cytosolic pH

Introduction

Real-time imaging of living cells is an important technique in cellular biochemistry research [1–5]. Recently, multi-labeling of samples has become common for obtaining richer information [6–9]. For instance, we can examine cell apoptosis and intracellular pH changes by labeling cells with both Annexin V-FITC and SNARF-1 [10]. The introduction of multi-fluorescent probes leads to severe spectral crosstalk in the data and affects the detection accuracy [11, 12]. The three-channel real-time fluorescence imaging method developed previously by our group can eliminate the majority of spectral crosstalk using three crosstalk indexes [10]. This method induces three crosstalk indexes and uses signal intensity to get corrected intensity of each channel. However the spectral distribution of most fluorescent probes is different, more crosstalk indexes are needed in the crosstalk matrix. In this work, we improved the efficiency of our three-channel real-time fluorescence imaging method in this respect, and the improved method was employed to detect early apoptotic events and intracellular pH changes in drug-treated thymus cells.

Z. Shu · L. Xiaochen · D. Chuyun · M. Wanyun (✉)
State Key Laboratory of Low-Dimensional Quantum Physics, Department of Physics, Tsinghua University, Beijing 100084, China
e-mail: mawy@mail.tsinghua.edu.cn

H. Man · P. Juhua · L. Xinghua · Q. Xin · D. Shaojin
Guang An Men Hospital, Beijing 100053, China

D. Chuyun
Science School, National University of Defense Technology, Changsha, Hunan 410073, China

M. Wanyun
Collaborative Innovation Center of Quantum Matter, Beijing, China

Methods

Improved Three-Channel Image Processing

Compared to the former method of eliminate the influence introduced by spectral crosstalk [10], introducing more crosstalk indexes into the crosstalk matrix may improve accuracy because of the spectral inhomogeneity of the probes. The intensity relationship between the three channels is as follows:

$$I_{Ch1} = I_{SF585} + a \cdot I_{AV535}, \quad (1)$$

$$I_{Ch2} = I_{SF655} + b \cdot I_{AV535}, \quad (2)$$

$$I_{Ch3} = I_{AV535} + c \cdot I_{SF585} + d \cdot I_{SF655}, \quad (3)$$

where I_{Ch1}, I_{Ch2}, I_{Ch3} are the signal intensities of the three detection channels. We used xenon lamp as the excitation

lamp (Sutter, American). The excitation wavelength is 300~650 nm. 585 nm and 655 nm are central wavelengths of two peaks in SNARF-1 fluorescence spectrum. I_{SF585}, I_{SF655} are the SNARF-1 intensities in channel 1 and channel 2, SF is the short name of SNARF-1. 535 nm is the central wavelength of peaks in FITC fluorescence spectrum. I_{AV535} is the Annexin V-FITC intensity in channel 3, AV is the short name of Annexin V-FITC, as shown in Table 1. I_{SF585}, I_{SF655}, I_{AV535} are corrected three-channel fluorescence intensities without spectral crosstalk. a, b, c, d are crosstalk indexes, which describe the level of spectral crosstalk in different channels. The intensity relationship can be rewritten as a matrix and vectors.

$$\begin{bmatrix} I_{Ch1} \\ I_{Ch2} \\ I_{Ch3} \end{bmatrix} = \begin{bmatrix} 1 & 0 & a \\ 0 & 1 & b \\ c & d & 1 \end{bmatrix} \begin{bmatrix} I_{SF585} \\ I_{SF655} \\ I_{AV535} \end{bmatrix} \quad (4)$$

or

$$\begin{bmatrix} I_{SF585} \\ I_{SF655} \\ I_{AV535} \end{bmatrix} = \begin{bmatrix} 1 & 0 & a \\ 0 & 1 & b \\ c & d & 1 \end{bmatrix}^{-1} \begin{bmatrix} I_{Ch1} \\ I_{Ch2} \\ I_{Ch3} \end{bmatrix} \quad (5)$$

Assuming that the change from single-labeling to double-labeling of samples does not affect spectral crosstalk in the three channels [10–12], the crosstalk indexes, a and b, can be calculated from the Annexin V-FITC single-labeled sample data. With Annexin V-FITC single-labeled, I_{SF655} and I_{SF585} should be zero, Then we can know from Eq. (4) that $a=I_{Ch1}/I_{Ch3}$, $b=I_{Ch2}/I_{Ch3}$. c and d can be obtained from the SNARF-1 single-labeled sample data as well.

Then, the corrected fluorescence intensities of the three channels can be derived from the crosstalk matrix in Eq. (5).

The value of I_{AV535} is proportional to the level of cell apoptosis. This is because in the process of apoptosis, phosphatidylserine turn over to the outside of the cell membrane. Annexin V-FITC specific binding with phosphatidylserine and emit fluorescence. So We use F to represent the value of I_{AV535}. A higher value of F means that the level of cell apoptos is higher.

SNARF-1 is a kind of special fluorescence probe which fluorescence spectrum related to the pH value of the environment. 655 nm and 585 nm are the central wavelength of two peak of SNARF-1fluorescence spectrum [13–15]. The two peaks intensity changes with intracellular pH. So $R=I_{SF655}/I_{SF585}$ can presents the intracellular pH value. A decreased R value indicates that the environmental pH of SNARF-1 has been reduced by cytosolic acidification [13–15].

Table 1 Description of Channels in Equation (1)–(3)

Symbol name	Description
I_{Ch1}	Original signal intensity in channel 1 (585 nm)
I_{Ch2}	Original signal intensity in channel 2 (655 nm)
I_{Ch3}	Original signal intensity in channel 3 (535 nm)
I_{SF585}	Corrected intensity of SNARF-1 in channel 1
I_{SF655}	Corrected intensity of SNARF-1 in channel 2
I_{AV535}	Corrected intensity of Annexin V in channel 3

Sample Preparation and Labeling

DCCM-2 medium was purchased from Biological Industries (Israel). Glutathione was purchased from Sigma Chemical (USA). The fluorescence indicators, Fluo-3/AM and Rhodamine 123 (Rh123), were purchased from Invitrogen (USA) and KeyGen Biotech. Co. (Nanjing, China), respectively. Ficoll lymphocyte separation medium (with a specific gravity of 1.092) was obtained from Hengxin Chemical Reagents (Shanghai, China). Phosphate-buffered saline (PBS) and D-Hank's buffer (without $CaCl_2$, $MgSO_4$ and phenolsulfonphthalein) were both acquired from Biosea Biotechnology (Beijing, China).

According to published data, GSNO, the reducing S-nitroso derivative of glutathione, must be freshly synthesized prior to being used in experiments. The mixture was protected from light throughout the procedure.

a) Preparation of thymocytes

Balb/c mice were purchased from the experimental animal center, CAS. The Annexin V-FITC cell apoptosis detection reagent kit was purchased from KENGEN Biotech. SNARF-1 was purchased from Invitrogen. GSH was purchased from Sigma.

Inbred BALB/C mice were purchased from the Experimental Animal Center of the Institute of Genetics and Developmental Biology, Academia Sinica (Beijing, China). Three-week-old mice with a mean weight of 12.5±0.9 g were sacrificed by cervical dislocation. The thymocytes were obtained by gently and repeatedly pressing the thymus against a

Table 2 Sample groups

Group	Drug treatment
Control 0 h	No treatment
Control	Buffer only, no drug
Control 3 h	Buffer only, no drug; incubated for 3 h
GSNO	0.3 mM GSNO
GSNO 3 h	0.3 mM GSNO; incubated for 3 h
GSNO+SRS	0.3 mM GSNO+127.14 $ng \cdot ml^{-1}$ SRS
GSNO+SRS 3 h	0.3 mM GSNO+127.14 $ng \cdot ml^{-1}$ SRS; incubated for 3 h
GSNO+PTIO	0.3 mM GSNO+200 μM PTIO
GSNO+PTIO 3 h	0.3 mM GSNO+200 μM PTIO; incubated for 3 h

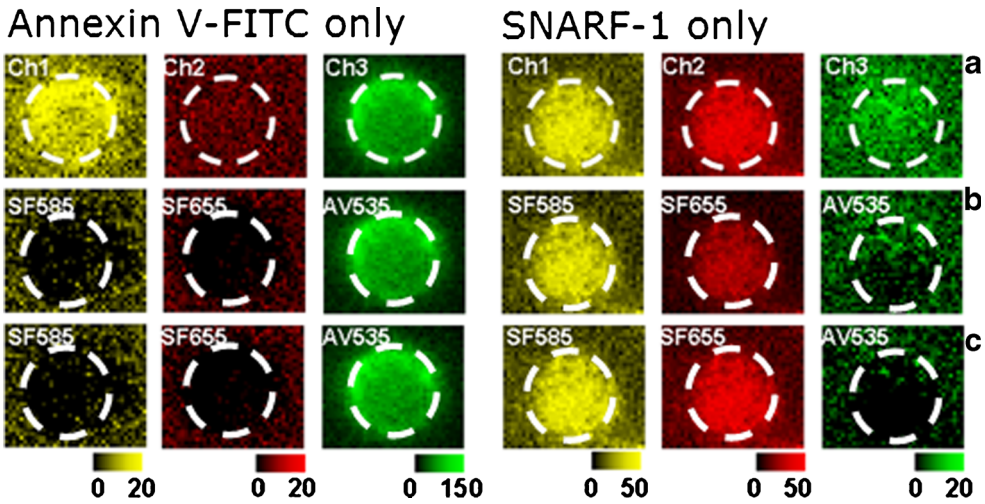

Fig. 1 Multi-labeling three-channel fluorescence image processing. **a** The first line – Original image **b** The second line — Original method. **c** The third line — Improved method. The *white dotted lines* indicate the area of the thymus cells

piece of nylon net submerged in D-Hank's buffer. Single cells were resuspended to 1×10^7 cells/ml in DCCM-2 medium and divided into aliquots for use. Three separate experiments were performed.

b) Labeling

To label the cells, they were washed with PBS and incubated with SNARF-1AM At 10 μmol $l\cdot l^{-1}$ for 15 min in the dark. After washing again with PBS, the cells were then incubated with Annexin V-FITC in the dark prior to imaging.

c) Sample groups

The description of each sample group is shown in Table 2.

Apoptosis Detection

The thymus cell suspensions (0.05 ml, 1×10^7 cells) were centrifuged for 5 min and washed twice with PBS (pH 7.38). Next, 500 μl of binding buffer, 5 μl of Annexin V-FITC and 5 μl of propidium iodide were added for every 5×10^5 cells and the samples were incubated at room temperature for 15 min in the dark.

The AV-PI labeled thymus cells were detected by flow cytometry (BD FACS Calibar, USA). Annexin V was detected with the channel FL 1 excitation/emission spectrum of 488/530 nm. PI was detected with the channel FL 2 excitation/emission spectrum of 488/650 nm.

Scatter plot data were acquired and analyzed using Summit software (BD FACS Calibar).

Statistical Analysis

SPSS Statistics 17.0 was used to analyze the data obtained from all groups. n indicates the number of cells analyzed (mean ± SEM).

The data were analyzed for statistical significance using a paired Student's *t*-test. The compiled data were expressed as the mean ± SEM, with n denoting the number of thymocytes analyzed.

Results and Discussion

Corrected Three-Channel Fluorescence Images

Figure 1 shows a comparison of the original image processing method with the improved method (The crosstalk indexes value is a=0.225, b=0.098, c=0.212, d=0.198). Figure 1a presents the original image with apparent spectral crosstalk, Fig. 1b is the image corrected using our previous method, and Fig. 1c is the image corrected using the improved method. The original method eliminated most of the crosstalk, as shown by comparing Fig. 1b with Fig. 1a. The improved method further eliminated the crosstalk, as shown by comparing Fig. 1c with

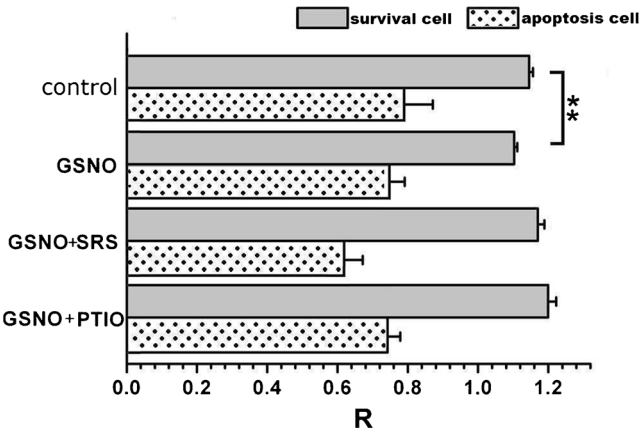

Fig. 2 The average value R (mean ± SEM) of survival cells and apoptosis cells in all groups. **p<0.01. (The cell number of each group is : control: n=125; GSNO: n=189; GSNO+SRS: n=139; GSNO+PTIO: n=164) SPSS Statistics 17.0 was used to analyze the data

Fig. 1b. This comparison shows that our improved method is more effective for AV535 crosstalk of SNARF-1.

Multi-label detection has become an important approach in the life sciences [6–9]. Spectral crosstalk is the main obstacle to quantifying experimental data, and eliminating crosstalk is the premise of quantified analysis of multi-labeling fluorescence signals [11, 12]. Our improved three-channel image processing method may effectively eliminate spectral crosstalk and make the quantification of three-channel fluorescence signals practicable. This method was applied to the observation of pH changes in mouse thymus cells during early apoptosis after treatment with different drugs.

Intracellular pH Changes in Mouse Thymus Cells Undergoing Apoptosis

Low concentrations of GSNO can induce mouse thymus cell apoptosis [16–18], while PTIO and SRS can inhibit apoptosis.

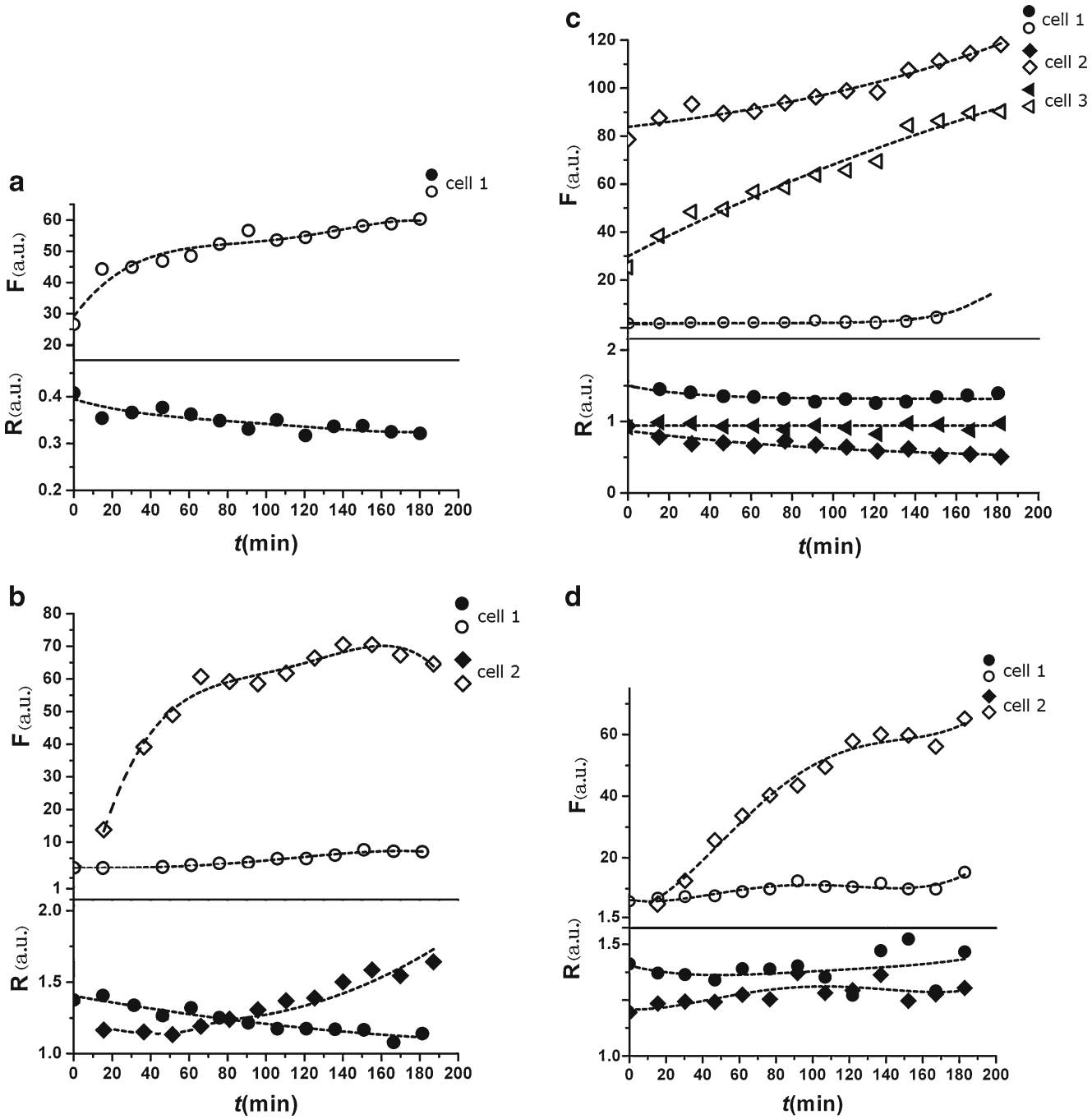

Fig. 3 Apoptosis and R value changes in drug-treated thymus cells. **a** control group **b** group adding GSNO **c** group adding GSNO+SRS **d** group adding GSNO+PTIO

Previously, the rate of apoptosis in GSNO-treated cells was shown to be higher than in control cells, thus demonstrating that GSNO can induce apoptosis [19]. In addition, the rate of apoptosis in GSNO+PTIO-treated cells was higher than in cells treated with GSNO only, indicating that PTIO also induces apoptosis. Furthermore, the rate of apoptosis in GSNO+SRS treated cells was slightly lower than in cells treated with GSNO only, indicating that SRS inhibits apoptosis.

The R values for apoptotic and normal cells are shown in Fig. 2. The R value of apoptotic cells was lower, indicating that the pH value was lower.

Real-Time Analysis of Apoptosis and pH Changes

Figure 3 shows typical data for all groups. Figure 3a shows that the intracellular pH decreases as apoptosis increases for normal apoptosis cells, consistent with the conclusions in "Intracellular pH Changes in Mouse Thymus Cells Undergoing Apoptosis". Figure 3b shows that the pH in cell 2 increased, which may indicate individual divergence. Figure 3c shows that the higher the level of apoptosis, the lower the intracellular pH. Cell 2 in Fig. 3d was undergoing apoptosis; its intracellular pH is lower. Here the R is not monotone. This indicated that process of apoptosis is complicated. We can only obtain the change trend in the progress. This also implied that only one index to estimate the level of apoptosis is not accurately. So with double-labeling we can estimate apoptosis with both R and F for which is better.

Conclusion

Our improved three-channel image processing method is more effective than the original method. The improved method was applied for observing early apoptosis and intracellular pH changes in mouse thymus cells. The results show that the pH values of apoptotic cells are lower than those of normal cells, and drug treatments affect the level of apoptosis.

Acknowledgments This work was supported by the National Nature Science Foundation of China (Grant Nos. 11374180 and 11174172), the Doctoral Program Research Fund of the Chinese Ministry of Education (Grant No. 20090002110065), and Tsinghua University Initiative Scientific Research Program (2010THZ01).

References

1. Huang Y, Fenech M, Shi Q (2011) Micronucleus formation detected by live-cell imaging. Mutagenesis 26(1):133–138
2. Maiuri P, Knezevich A, Bertrand E, Marcello A (2011) Real-time imaging of the HIV-1 transcription cycle in single living cells. Methods 53:62–67
3. Lee S, Choi KY, Chung H et al (2011) Real time, high resolution video imaging of apoptosis in single cells with a polymeric nanoprobe. Bioconjug Chem 22:125–131
4. Seo JH, Cho K, Lee SY, Joo S (2011) Concentration-dependent fluorescence live-cell imaging and tracking of intracellular nanoparticles. Nanotechnology 22:235101
5. Hotzer B, Ivanov R, Brumbarova T, Bauer P, Jung G (2012) Visualization of Cu2+ uptake and release in plant cells by fluorescence lifetime imaging microscopy. FEBS J 279:410–419
6. Shroff H, Galbraith CG, Galbraith JA et al (2007) Dual-color super resolution imaging of genetically expressed probes within individual adhesion complexes. PNAS 104(51):20308–20313
7. Togashi DM, Ryder AG (2010) Assessing protein-surface interactions with a series of multi-labeled BSA using fluorescence lifetime microscopy and Forster Energy Resonance Transfer. Biophys Chem 52:55–64
8. Buckers J, Wildanger D, Vicidomini G, Kastrup L, Hell SW (2011) Simultaneous multi-lifetime multi-color STED imaging for colocalization analyses. Opt Express 19(4):3130–3143
9. Butko MT, Drobizhev M, Makarov NS et al (2011) Simultaneous multiple-excitation multiphoton microscopy yields increased imaging sensitivity and specificity. BMC Biotechnol 11:20
10. Lin D, Liu X, Ma W (2009) Study of the relationship between apoptosis and intracellular pH in single living cells using a three-channel real-time fluorescence imaging method. Spectrosc Spectr Anal 29(6):1581–1585
11. Elangovan M, Wallrabe H, Chen Y et al (2003) Characterization of one- and two-photon excitation fluorescence resonance energy transfer microscopy. Methods 29(1):58–73
12. Wallrabe H, Periasamy A (2005) Imaging protein molecules using FRET and FLIM microscopy. Curr Opin Biotechnol 16(1):19–27
13. Buckler KJ, Vaughan-Jones RD (1990) Application of a new pH-sensitive fluoroprobe (carboxy-SNARF-1) for intracellular pH measurement in small, isolated cells. Pflugers Arch - Eur J Physiol 417(2):234–239
14. Seksek O, Henry-Toulme N, Sureau F, Bolard J (1991) SNARF-1 as an intracellular pH indicator in laser microspectrofluorometry: a critical assessment. Anal Biochem 193(1):49–54
15. Wieder ED, Hang H, Fox MH (1993) Measurement of intracellular pH using flow cytometry with carboxy-SNARF-1. Cytometry 14(8): 916–921
16. Sandau K, Brune B (1996) The dual role of S-nitrosoglutathione (GSNO) during thymocyte apoptosis. Cell Signal 8(3):173–177
17. Lin D, Ma W, Duan S, Zhang Y, Du L (2006) Real-time imaging of viable-apoptotic switch in GSNO-induced mouse thymocyte apoptosis. Apoptosis 11(8):1289–1298
18. Duan S, Wan L, Fu W et al (2009) Nonlinear cooperation of p53-ING1-induced bax expression and protein S-nitrosylation in GSNO-induced thymocyte apoptosis: a quantitative approach with cross-platform validation. Apoptosis 14(2):236–245
19. Duan S, Gu L, Zhang C et al (2006) Radish seed sinapine delay thymocyte cell apoptosis induced by GSNO. Academic conference proceedings of the sixth China medicine institute. pp 5175–5198